Amit KUMAR [1], Krishna Prasad MADASU [1]

Non-Newtonian fluid flow between parallel plates filled with an anisotropic porous medium

Micropolar fluid flow through an anisotropic porous medium between two horizontally oriented impermeable plates under the effect of slip conditions for velocity and microrotation vectors at both plates are analysed in this paper. The permeability of an anisotropic porous medium is along two principal axes of permeability K_1 and K_2. The principal axis with permeability K_2 forms an angle ψ with the horizontal direction called anisotropic (or orientation) angle. It is observed that the velocity and the microrotation profiles decrease as permeability ratio K and orientation angle ψ increase. Velocity slip (β_1 and β_2) parameters show the effect on the velocity profile near upper and lower plates but have a strong influence on the microrotation profile. The spin slip (σ_1 and σ_2) parameters showed minor enhancement in the velocity profile but had an increasing effect on the microrotation vector. The decrease in permeability ratio and anisotropic angle results in an increase in skin friction. The impact of other parameters like Darcy number Da, micropolar parameter N on velocity and microrotation vectors are presented graphically and discussed. The presence of the slip effect helps to reduce the impact of friction due to plates causing fluid flow to enhance.

Nomenclature

u	velocity in the x- direction
ν	microrotation angular velocity
x, y	Cartesian coordinates along the channel
h	dimensionless height
μ	dynamic viscosity coefficient of the fluid
κ	rotational viscosity coefficients
p	pressure term
$\alpha_0, \beta_0, \gamma_0$	coefficients of gyro-viscosity of the micropolar fluid

✉ Krishna Prasad MADASU, email: madaspra.maths@nitrr.ac.in, kpm973@gmail.com

[1] National Institute of Technology Raipur, Raipur, Chhattisgarh, India.
   A.K. email: akumar.phd2022.maths@nitrr.ac.in

K_{pm}	second order permeability tensor
K_1, K_2	permeability along principal axes
ψ	anisotropic angle
β_1, β_2	velocity slip parameters
σ_1, σ_2	spin slip parameters
V_0	average velocity
N	micropolarity parameter
p_0	dimensionless pressure term
Γ_1, Γ_2	dimensionless velocity slip parameters
λ_1, λ_2	dimensionless spin slip parameters
u_∞	velocity at large Darcy number
v_∞	microrotation at large Darcy number
C_f, m_f	skin-friction coefficients of stress and couple stress

1. Introduction

The occurrence of fluid flow through a porous media is widespread in natural and industrial fields like water label recharge, oil recovery, water filtration plants, and nuclear power plants [1]. The presence of microstructure makes non-Newtonian flow patterns different from the classical Newtonian fluid inside a porous medium, and it has a significant role in industries, including chemical, polymer, and biomedical [2]. A fluid with characteristics different from Newtonian and non-Newtonian fluids is a nanofluid, with nanoparticles (gold, silver, copper, and platinum) inside the fluid. Its major applications include renewable energy engineering, transportation, medical fields, aircraft, heat transport enhancement, and microelectronics [3, 4]. These applications and the behaviour of fluid motion in porous mediums attract many researchers to investigate the problem related to porous mediums. The key factors porosity and permeability characterize the flow in a porous medium, and they strongly affect the rheological properties of Newtonian, non-Newtonian, and nanofluid. The isotropic porous structure has constant permeability, but the permeability of the homogenous anisotropic structure depends on the porous lining arrangement.

Most natural and manufactured porous materials, like sand, rocks, tree trunks, and porous layer arteries, are heterogeneous in structure. The permeability in these materials is different in all directions. In 1991, Tyvand and Storesletten introduced the term inclination angle to study the onset of Rayleigh–Bénard convection in a bounded horizontal porous medium of anisotropic nature [5]. They consider the arbitrary manner of porous lining to form an angle with the horizontal direction, which is common in the whole material. This angle is known as the inclination angle or anisotropic angle [5]. Introducing an angle makes the permeability differ in $x-$ and $y-$ directions and vary with the inclination angle (see Fig. 1). Degan et al. [6] introduced the inclination angle in a horizontal porous medium to study the effect of anisotropic parameters on the forced convective flow. Karmakar and Raja Shekhar [7] have done a detailed analysis of the influence of anisotropic

parameters on fluid flow between two porous channels. Recently, Israel-Cookey et al. [8] investigated the forced convective flow of an electrically conducting Casson fluid through an anisotropic porous channel. They observed that with a decrease in permeability ratio, fluid activity increases. They found that the anisotropic structure of porous medium provides greater insight than an isotropic structure.

A micropolar fluid flow mechanism is different from a classical Newtonian fluid. Eringen [9] introduced the concept of micropolar fluid to describe the behaviour of fluids like animal blood, muddy water, lubricants, and polymeric suspensions. A review article on the wide range of micropolar fluid applications proposed by Ariman et al. [10]. Some selected applications of micropolar fluid in porous mediums and lubrication theory can be found in Lukaszewicz's textbook [11]. Ariman and Cakmak [12] investigated micropolar fluid Couette, Poiseuille, and rotating flows. Analytical solutions for the impact of MHD on the time-dependent boundary layer flow of a micropolar fluid were given by Nadeem et al. [13]. Pandey and Chaube [14] examined magnetically influenced micropolar fluid flow inside a porous media induced by a peristaltic sinusoidal wave. Madasu and Bucha [15] studied the effect of MHD on a cylinder placed in a porous medium filled with micropolar fluid. Hydromagnetic effect on free convective flow and mixed convective fluid flow through different geometries governed by non-Darcy model are investigated by Chamkha [16, 17]. Chamkha [18, 19] studied electromagnetic two-phase flow through horizontal channels and circular pipes. Chamkha [20] analytically solved and verified numerically the free convective flow of a micropolar fluid through the vertical channel and studied the MHD effect on mixed convective flow in the same geometry with different thermal conditions [21]. The flow behaviour of immiscible fluid in non-porous and porous channels with and without magnetic effect was studied by Chamkha [22]. Time-dependent immiscible fluid flow and heat transfer in horizontal channels [23] and free convective flow of immiscible fluid in vertical channels [24] are also investigated. Keimanesh et al. [25] studied the generalized Couette flow of a third-grade non-Newtonian fluid and all its cases. MHD effect on micropolar fluid flow through an isotropic porous medium studied by Kocić et al. [26]. Ahmad and Rashad [27] studied the natural convective flow of micropolar nanofluid inside the rectangular anisotropic porous enclosure.

Navier [28, 29] has introduced more practical slip boundary conditions, where slippage occurs along the boundary's surface. The slip condition assumes that the tangential velocity of the fluid particles at a boundary point is proportional to the tangential stress acting at that moment of contact. Neto et al. [30] have given a summary of their research on the experimental investigation of Newtonian fluid boundary slip conditions. The presence of wall slip can have beneficial effects, such as reducing the required pressure drop in microfluidic applications [31, 32]. The wall slip effect on fluid flow and heat transfer through a porous medium has been studied by Ramesh [33]. Chen et al. [34] used the Navier slip condition to study non-Newtonian fluid flows over channelled surfaces. Slayi and Ashmawy [35] investigated the time-dependent flow of micropolar fluid flow with velocity and

spin slip between two parallel plates. Madasu and Sarkar [36] studied the effect of slip conditions on a sphere implanted in a porous medium of constant permeability saturated with a couple of stress fluids. Bucha and Madasu [37] worked on the effect of slip conditions on flow past a permeable spheroid confined inside a spheroidal cell with isotropic permeability. Only a few studies have employed an anisotropic porous channel with slip boundary conditions. Jingang [38] investigated anisotropic velocity slip at the interface of a unidirectional fibrous porous medium using Navier's slip condition. Abdelsalam et al. [2] did a comparative study on the MHD effect on a Maxwell fluid flow and heat transfer through a porous medium with a slip effect. Karmakar [39] investigated the unsteady Couette flow of Newtonian fluid through an anisotropic porous media confined by two parallel plates; the roughness of the lower plate causes a slip.

The excellent understanding of the velocity profile for different Newtonian and non-Newtonian fluids inside an anisotropic porous medium and the effect of slip boundary condition case motivates us to do the present study. Slips occur because of the nature of the plate's surface and fluid; microparticles of micropolar fluid also affect the flow [40]. We believe that using slip boundary conditions for both velocity and microrotation are more physical. Nowadays, various types of artificial porous metallic lattice structures like the diamond orientation of a stainless steel textile sandwich panel [41], octahedral lattice material of a casting aluminium alloy [42], and solid and hollow microtruss lattice structures [43] are available. But these materials have some limitation due to the size of pores. Nanoporous metal foams are also manmade porous materials finer than porous lattice structures used in particular electrodes, sensors, and filters [44]. Furthermore, these metal foams can be viewed as suitable for use in high-speed conduction and catalyst materials that have very large specific surface areas [45]. The adjustment of their permeability in different directions based on needs are the major advantage of these artificial foams or porous materials. These materials have many potential applications in engineering and industrial fields, like in filtration, making of biomaterials, etc. The present study is helpful in exploring the behaviour of fluid flow in these artificial porous structure.

The current problem involved analyzing the flow of micropolar fluid through an anisotropic porous medium. Slip boundary conditions are considered for velocity and microrotation vectors at upper and lower impermeable plates. The most important findings about the effect of velocity slip, spin slip, anisotropic permeability, Darcy number and micropolarity parameter on the velocity and microrotation profiles have been mentioned.

2. Problem formulation

The equations governing the laminar and steady flow of an incompressible micropolar fluid with constant fluid properties through a porous medium, in the absence of body force and body couple are given as follows [14, 15]

$$\nabla \cdot \mathbf{q} = 0, \tag{1}$$

$$\nabla p + (\mu + \kappa)\mathbf{K}_{pm}^{-1}\mathbf{q} + (\mu + \kappa)\nabla \times \nabla \times \mathbf{q} - \kappa\nabla \times \mathbf{v} = 0, \tag{2}$$

$$\kappa\nabla \times \mathbf{q} - 2\kappa\mathbf{v} - \gamma_0\nabla \times \nabla \times \mathbf{v} + (\alpha_0 + \beta_0 + \gamma_0)\nabla(\nabla \cdot \mathbf{v}) = 0, \tag{3}$$

where $\mathbf{q}$, $\mathbf{v}$, μ, κ, p, $\mathbf{K}_{pm}$ are the velocity vector, microrotation vector, coefficient of viscosity for the viscous fluid, rotational viscosity coefficients, pressure, and permeability tensor, respectively. α_0, β_0, γ_0 are the coefficients of gyro-viscosity of the micropolar fluid.

The stress and couple stress tensors are described by

$$\mathbf{t}_{ij} = -p\delta_{ij} + \mu(\mathbf{q}_{i,j} + \mathbf{q}_{j,i}) + \kappa(\mathbf{q}_{j,i} - \epsilon_{ijm}\mathbf{v}_m), \tag{4}$$

$$\mathbf{m}_{ij} = \alpha_0\mathbf{v}_{m,m}\delta_{ij} + \beta_0\mathbf{v}_{i,j} + \gamma_0\mathbf{v}_{j,i}, \tag{5}$$

where ϵ_{ijm} and δ_{ij} are the alternating tensor, and Kronecker delta, respectively and the comma denotes the covariant differentiation.

Consider the fully developed flow of micropolar fluid (i.e., transverse velocity is zero, $u = u(y)$ and $v = v(y)$ [14, 15]) through an anisotropic porous medium between two horizontal parallel impermeable plates (see Fig. 1). Width of the plates along the z−direction to be infinitely large as compared to its height ($2h$). So that, flow variables along the z−direction, i.e., $w = 0$, $\dfrac{\partial w}{\partial z} = 0$.
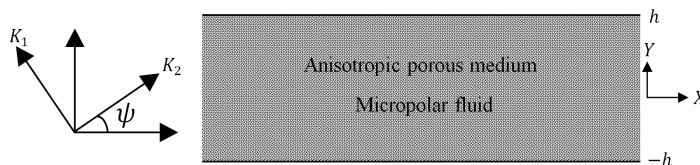
Fig. 1. Schematic presentation

The permeability of the porous medium is along the principal axis of permeability K_1 and K_2, and the principal axis of permeability K_2 makes an angle with ψ with the horizontal axis. The permeability ratio $\left(K = \dfrac{K_1}{K_2}\right)$ and orientation angle ψ described the anisotropy of the porous region. Then, the permeability $\mathbf{K}_{pm}$ of an anisotropic porous medium is the second-order tensor and given by [5–8, 27, 39]

$$\mathbf{K}_{pm} = \begin{bmatrix} K_1\sin^2\psi + K_2\cos^2\psi & (K_2 - K_1)\sin\psi\cos\psi \\ (K_2 - K_1)\sin\psi\cos\psi & K_2\sin^2\psi + K_1\cos^2\psi \end{bmatrix}. \tag{6}$$

When $K = 1$ i.e., $K_1 = K_2$, it is the case of isotropic porous medium.

With the above consideration the governing equations Eq. (1)-(3) reduce to

$$\frac{\partial u}{\partial x} = 0, \tag{7}$$

$$\frac{\partial p}{\partial x} + \frac{(\mu + \kappa)}{K_1} au - (\mu + \kappa)\frac{\partial^2 u}{\partial y^2} - \kappa\frac{\partial v}{\partial y} = 0, \tag{8}$$

$$\frac{\partial p}{\partial y} + \frac{(\mu + \kappa)}{K_1} bu = 0, \tag{9}$$

$$-\kappa\frac{\partial u}{\partial y} - 2\kappa v + \gamma_0\frac{\partial^2 u}{\partial y^2} = 0, \tag{10}$$

where $a = \sin^2 \psi + K \cos^2 \psi, \ b = (K - 1)\sin\psi\cos\psi,$ (11)

with the slip boundary conditions for velocity and microrotation vectors [35, 40]

$$\beta_1 u = (\mu + \kappa)\frac{\partial u}{\partial y} + \kappa v, \quad \sigma_1 v = \gamma_0\frac{\partial v}{\partial y} \text{ at } y = -h, \tag{12}$$

$$\beta_2 u = -(\mu + \kappa)\frac{\partial u}{\partial y} - \kappa v, \quad \sigma_2 v = -\gamma_0\frac{\partial v}{\partial y} \text{ at } y = h, \tag{13}$$

where $0 \leqslant \beta_1, \beta_2 < \infty$ are the velocity slip parameters, and $0 \leqslant \sigma_1, \sigma_2 < \infty$ spin slip parameters.

Now, partially differentiate Eq. (8) and (9) with respect to x and using Eq. (7), we obtain

$$\frac{\partial}{\partial x}\left(\frac{\partial p}{\partial x}\right) = 0 \quad \text{and} \quad \frac{\partial}{\partial y}\left(\frac{\partial p}{\partial x}\right) = 0. \tag{14}$$

According to Karmakar [7], and from Eq. (14), it follows that,

$$\frac{\partial p}{\partial x} = Q. \tag{15}$$

From Eq. (8) and (9), we can say that the anisotropic parameters affects the change in pressure gradient in both x and y directions.

The average velocity V_0 through the channel, can be evaluated using volumetric flow (V_{total}) per unit width of the channel [7], i.e.,

$$V_0 = \frac{V_{\text{total}}}{2h} = \frac{1}{2h}\left(\int_{-h}^{h} u \, dy\right). \tag{16}$$

The expressions of tangential stress and tangential couple stress are given by

$$\tau_{yx} = (\mu + \kappa)\frac{\partial u}{\partial y} + \kappa v, \quad m_{yz} = \gamma_0\frac{\partial v}{\partial y}. \tag{17}$$

3. Analytical solution

Using the following dimensionless parameters,

$$u^* = \frac{u}{V_0}, \quad v^* = \frac{vh}{V_0}, \quad x^* = \frac{x}{h}, \quad y^* = \frac{y}{h}, \quad p^* = \frac{p}{p_0}, \quad p_0 = \frac{(\mu + \kappa)V_0}{h}, \tag{18}$$

and after dropping the $(*)$, the resulting dimensionless equations are

$$\frac{\partial^2 u}{\partial y^2} + l\frac{\partial v}{\partial y} - \frac{a}{\mathrm{Da}}u - Q = 0, \tag{19}$$

$$\frac{\partial p}{\partial y} + \frac{b}{\mathrm{Da}}u = 0, \tag{20}$$

$$\frac{\partial^2 v}{\partial y^2} - f\frac{\partial u}{\partial y} - 2fv = 0, \tag{21}$$

where $N = \dfrac{\kappa}{\mu}$, $l = \dfrac{N}{1+N}$, $f = \dfrac{\kappa h^2}{\gamma_0}$, $\mathrm{Da} = \dfrac{K_1}{h^2}$.

And corresponding slip boundary conditions are

$$\Gamma_1 u = (1+N)\frac{\partial u}{\partial y} + Nv, \quad \lambda_1 v = \frac{\partial v}{\partial y} \ \text{ at } \ y = -1, \tag{22}$$

$$\Gamma_2 u = -(1+N)\frac{\partial u}{\partial y} - Nv, \quad \lambda_2 v = -\frac{\partial v}{\partial y} \ \text{ at } \ y = 1, \tag{23}$$

where $\Gamma_1 = \dfrac{\beta_1 h}{\mu}$, $\lambda_1 = \dfrac{\sigma_1 h}{\gamma_0}$, $\Gamma_2 = \dfrac{\beta_2 h}{\mu}$, $\lambda_2 = \dfrac{\sigma_2 h}{\gamma_0}$.

The velocity and microrotation vectors after solving the Eq. (19) and Eq. (21) are

$$u = c_1 e^{-\eta y} + c_2 e^{\eta y} + c_3 e^{-\xi y} + c_4 e^{\xi y} - \frac{Q}{\alpha^2}, \tag{24}$$

$$v = \frac{\alpha^2 - \eta^2}{l\eta}(-c_1 e^{-\eta y} + c_2 e^{\eta y}) + \frac{\alpha^2 - \xi^2}{l\xi}(-c_3 e^{-\xi y} + c_4 e^{\xi y}), \tag{25}$$

where $\eta = \dfrac{\sqrt{(\alpha^2 + (2-l)f) + \sqrt{(\alpha^2 + (2-l)f)^2 - 8\alpha^2 f}}}{\sqrt{2}}$,

$\xi = \dfrac{\sqrt{(\alpha^2 + (2-l)f) - \sqrt{(\alpha^2 + (2-l)f)^2 - 8\alpha^2 f}}}{\sqrt{2}}$, and $\alpha = \sqrt{\dfrac{a}{\mathrm{Da}}}$.

In which c_1, c_2, c_3, c_4 can be evaluated using above boundary conditions.

The nondimensional form of balanced volume flow is given below

$$1 = \frac{1}{2}\left(\int_{-1}^{1} u \, \mathrm{d}y \right). \tag{26}$$

Note that the pressure gradient Q can be obtained using Eq. (26). The Eq. (26) also represents the conservation of volume flux.

The dimensionless skin-friction coefficients are given by [40]

$$C_f = \pm \frac{\dfrac{\mathrm{d}u}{\mathrm{d}y} + lv}{Q}|_{y=\mp 1}, \tag{27}$$

$$m_f = \pm \frac{\dfrac{l}{f}\dfrac{\mathrm{d}v}{\mathrm{d}y}}{Q}|_{y=\mp 1}, \tag{28}$$

where the plus and minus signs correspond to the upper and lower plates, respectively.

4. Results and discussion

The effect of different parameters like permeability ratio K, anisotropic angle ψ, velocity slip parameters (Γ_1 and Γ_2), microrotation slip parameters (λ_1 and λ_2), micropolar parameter N, and Darcy number Da on velocity profile and microrotation are presented in this part.

Figs. 2 and 3 show the effect of permeability ratio and orientation angle on fluid velocity. As Da < 1, (i.e., fixed K_1) and $\psi = 0$ then with an increase in permeability ratio K, permeability along the flow direction decreases, causing velocity decreases, as shown in Fig. 2. The velocity achieves maximum at the channel's centerline and slows down near the plates due to the presence of viscous term but does not reach zero due to the slip effect of plates. For $K < 1$(i.e., $K_1 < K_2$), the velocity decreases as the inclination angle (ψ) increases because the permeability along the
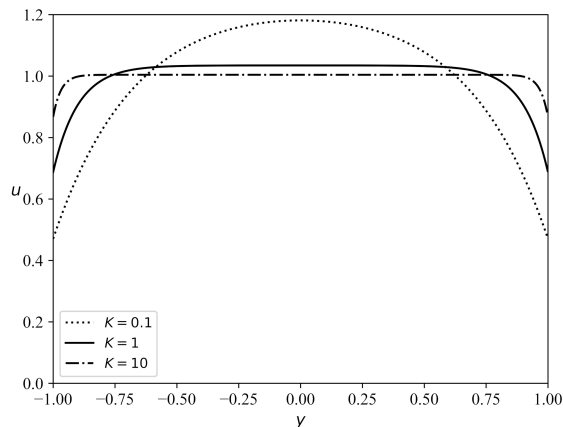
Fig. 2. Impact of permeability ratio on velocity when
Da $= 0.01, N = f = 1, \psi = 0, \Gamma_1 = \Gamma_2 = \lambda_1 = \lambda_2 = 10$
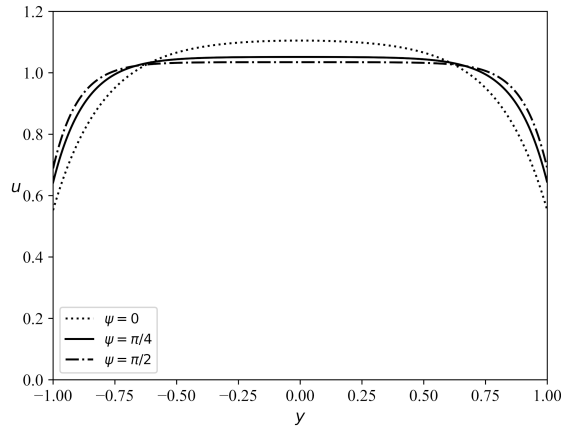
Fig. 3. Impact of anisotropic angle on velocity when
$Da = 0.01, N = f = 1, K = 0.25, \Gamma_1 = \Gamma_2 = \lambda_1 = \lambda_2 = 10$

flow direction decreases, as shown in Fig. 3. At $\psi = 0$, the principal axis with low permeability is parallel to the $y-$axis, causing velocity to achieve maximum and minimum at $\psi = \dfrac{\pi}{2}$, the same behaviour observed by others [6, 7, 39]. The opposite behaviour is seen, when $K > 1$, i.e., velocity is maximum at $\psi = \dfrac{\pi}{2}$ and minimum at $\psi = 0$ [6, 7, 39]. For flow, the required pressure gradient is obtained using Eq. (26), this equation also represents the balanced volume flow throughout the channel [7]. Most of the available studies showed that flow in an isotropic porous medium is due to some constant pressure gradient in every case of permeability. First time, this concept is used by Karmakar and Raja Shekhar [7]. If we use balanced volume case then, it helps to understand more about pressure and permeability relation. Table 1 and Table 2 mention the difference in V_{total} for different permeability ratios and anisotropic angles for fixed $Q = -3, -5, -7$ and the assumption of constant V_{total} of the present problem.

Table 1. Comparison of V_{total} of the present problem with fixed Q
for different permeability ratios

Permeability ratio	$K = 0.1$	$K = 1$	$K = 10$
V_{total} (of present study)	1.99999	2.0	2.0
V_{total} for (fixed $Q = -3$)	0.48574	0.058006	0.00597
V_{total} for (fixed $Q = -5$)	0.80956	0.09667	0.00995
V_{total} for (fixed $Q = -7$)	1.13339	0.13534	0.01393

We consider the $\Gamma_1 = \Gamma_2$ and $\lambda_1 = \lambda_2$ to study the velocity slip and spin slip parameter's influence on velocity profile, respectively. The velocity slip parameters Γ_1 and Γ_2 enhanced the flow near plates (see Fig. 4). It is observed that for $\Gamma_1 = \Gamma_2 = 0.01$, velocity is maximum at the lower and upper plates, and as $\Gamma_1 \to \infty, \Gamma_2 \to \infty$, i.e., no-slip condition, velocity at plates is least. However, this

Table 2. Comparison of V_{total} of the present problem with fixed Q
for different anisotropic angles

Anisotropic angle	$\psi = 0$	$\psi = \dfrac{\pi}{4}$	$\psi = \dfrac{\pi}{2}$
V_{total} (of present study)	1.99999	2.0	1.99999
V_{total} for (fixed $Q = -3$)	0.21612	0.09130	0.058003
V_{total} for (fixed $Q = -5$)	0.36020	0.15217	0.09667
V_{total} for (fixed $Q = -7$)	0.50428	0.21305	0.13534
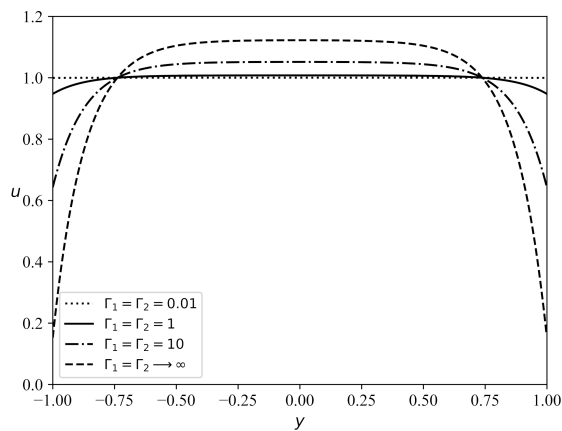
Fig. 4. Impact of velocity slip on velocity when
$Da = 0.01, N = 1, f = 1, K = 0.25, \lambda_1 = \lambda_2 = 10, \psi = \dfrac{\pi}{4}$
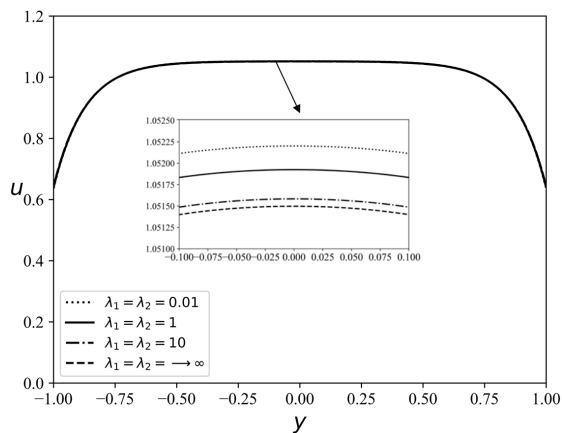
Fig. 5. Impact of spin slip on velocity when
$Da = 0.01, N = 1, f = 1, K = 0.25, \psi = \dfrac{\pi}{4}, \Gamma_1 = \Gamma_2 = 10$

happens near the plates only; in the channel's centerline, the flow is at its maximum for the no-slip condition. It is depicted from Fig. 5, that a very small enhancement in velocity happens due to an increase in spin slip parameters λ_1 and λ_2.

The velocity decreases as micropolar parameter N increases (see Fig. 6). When $N = \dfrac{\kappa}{\mu} = 0$, then it represent the Newtonian case. For the present problem, when $N = 0.0001$, it behaves like the Newtonian case. Fig. 7 discloses the effect of Darcy number on fluid's velocity, and Figs. 8 and 9 disclose the influence of Darcy number on pressure gradient varying in the $y-$direction with slip and no-slip case, respectively. As the Darcy number increases, the permeability along the flow direction increases. Hence, velocity increases and pressure along the $y-$direction
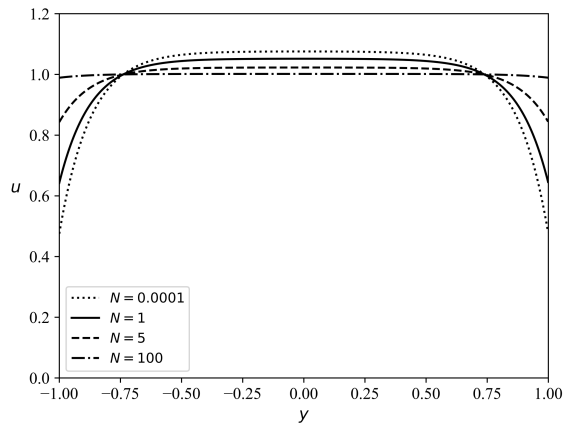
Fig. 6. Impact of micropolar parameter on velocity when
$\mathrm{Da} = 0.01, K = 0.25, \psi = \dfrac{\pi}{4}, \Gamma_1 = \Gamma_2 = \lambda_1 = \lambda_2 = 10, f = 1$
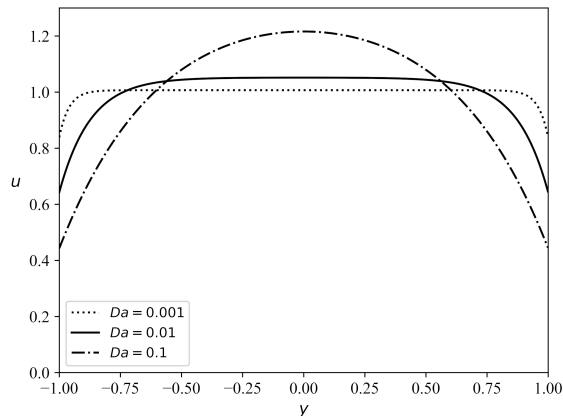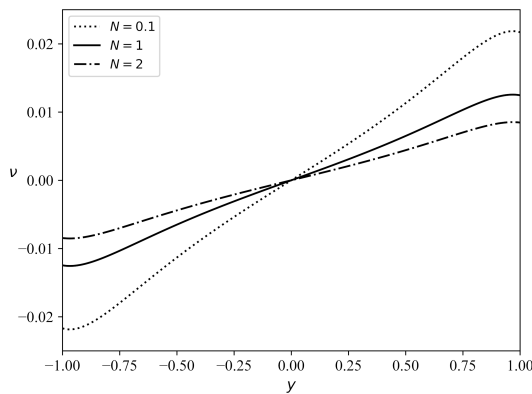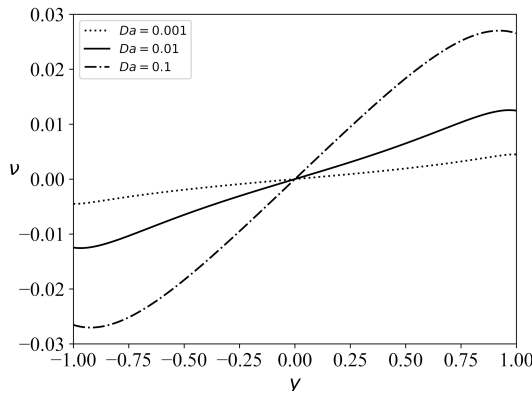

Fig. 7. Impact of Darcy number on velocity when
$f = 1, N = 1, K = 0.25, \psi = \dfrac{\pi}{4}, \Gamma_1 = \Gamma_2 = \lambda_1 = \lambda_2 = 10$
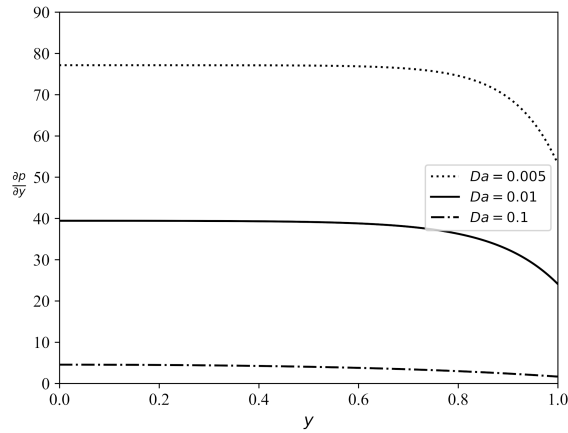
Fig. 8. Impact of Darcy number on vertical pressure gradient when
$N = 1, f = 1, K = 0.25, \psi = \dfrac{\pi}{4}, \Gamma_1 = \Gamma_2 = \lambda_1 = \lambda_2 = 10$
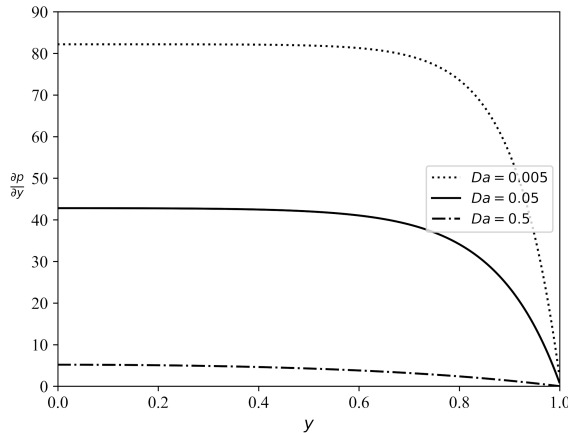
Fig. 9. Impact of Darcy number on vertical pressure gradient when
$N = 1, f = 1, K = 0.25, \psi = \dfrac{\pi}{4}, \Gamma_1 = \Gamma_2 = \lambda_1 = \lambda_2 = 1000$

decreases. For Da $= 0.1$, it is very close to parabolic, it represent clear flow of micropolar fluid. It is found that, when Da < 0.1, then flow increases with increase in permeability.

The impact of permeability ratio K and orientation angle ψ, micropolar parameter N, Darcy number Da, velocity slip parameters (Γ_1 and Γ_2), and microrotation slip parameters (λ_1 and λ_2) on microrotation are shown in Figs. 10–15, respectively.

The microrotation profile decreases with an increase in the permeability ratio and the anisotropic angle. This is due to the permeability along the flow decreases with an increase in the permeability ratio and anisotropic angle. The microrotation increases as permeability increases with the rise in Darcy number along the flow
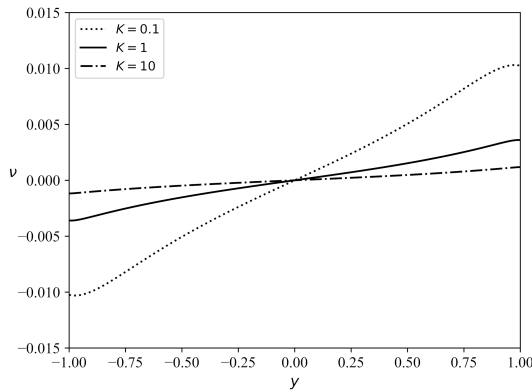
Fig. 10. Impact of permeability ratio on microrotation when
$Da = 0.001, \psi = 0, N = f = 1, \Gamma_1 = \Gamma_2 = \lambda_1 = \lambda_2 = 0.5$
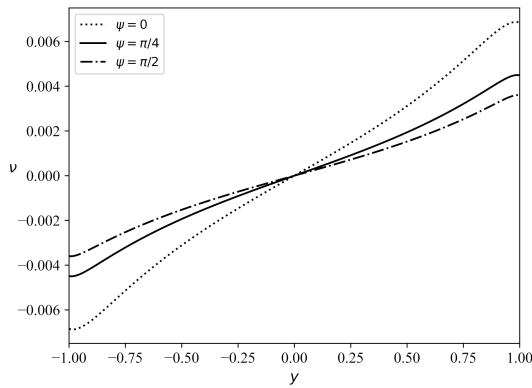
Fig. 11. Impact of anisotropic angle on microrotation when
$Da = 0.001, K = 0.25, N = f = 1, \Gamma_1 = \Gamma_2 = \lambda_1 = \lambda_2 = 0.5$

Fig. 12. Impact of micropolar parameter on microrotation when
$Da = 0.001, f = 1, K = 0.25, \psi = \dfrac{\pi}{4}, \Gamma_1 = \Gamma_2 = \lambda_1 = \lambda_2 = 0.5$

Fig. 13. Impact of Darcy number on microrotation when
$N = f = 1, K = 0.25, \psi = \dfrac{\pi}{4}, \Gamma_1 = \Gamma_2 = \lambda_1 = \lambda_2 = 0.5$
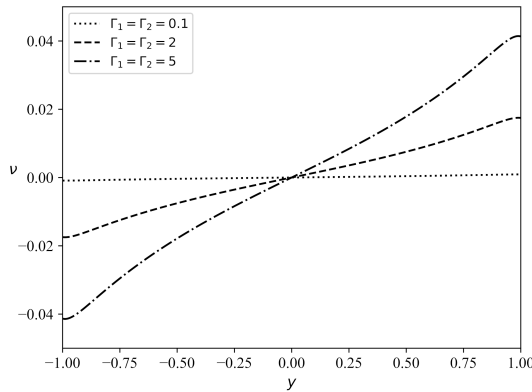
Fig. 14. Impact of velocity slip on microrotation vector when
$Da = 0.001, K = 0.25, N = f = 1, \psi = \dfrac{\pi}{4}, \lambda_1 = \lambda_2 = 0.5$
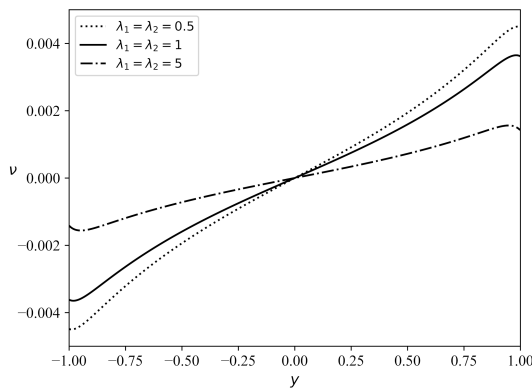
Fig. 15. Impact of spin slip on microrotation vector when
$Da = 0.001, K = 0.25, \psi = \dfrac{\pi}{4}, N = f = 1, \Gamma_1 = \Gamma_2 = 0.5$

direction. The additional viscosity (κ) effects the characteristics of micropolar fluid [26]. The micropolarity parameter (N) increases, which means that (κ) increases because μ is fixed, causing a microrotation profile decrease. With an increase in the velocity slip parameter, microrotation increases but decreases with an increase in the spin slip parameter.

Figs. 16 and 17 show the effect of permeability ratio and anisotropic angle on skin friction of stress with respect to Darcy's number, respectively. Skin friction in case of Newtonian fluid ($N = 0$, $f = 0$) is greater than micropolar fluid. As the permeability ratio increases, it causes velocity decreases (as explain above); hence, the skin friction decreases. The same behaviour have also observed by Karmakar [39]. And Figs. 18 and 19 represent the skin friction of couple stress on an upper plate with respect to Darcy's number. It also shows that skin friction increases with an increase in flow.
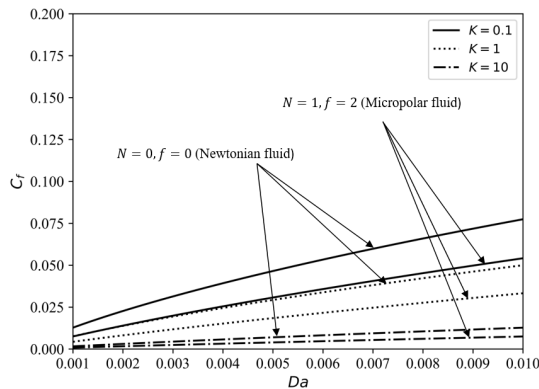
Fig. 16. Impact of permeability ratio on skin friction of stress for
Newtonian fluid ($N = 0$, $f = 0$) and micropolar fluid ($N = 1$, $f = 2$)
on upper plate when $\psi = 0$, $\Gamma_1 = \Gamma_2 = \lambda_1 = \lambda_2 = 10$
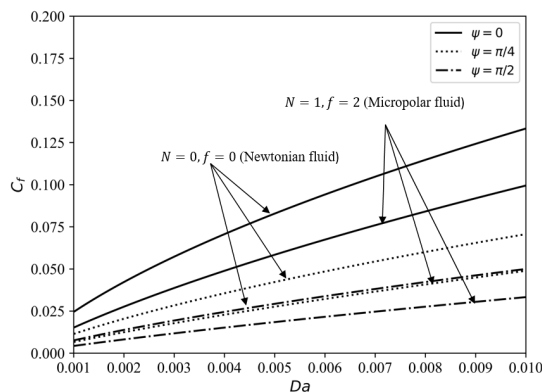
Fig. 17. Impact of anisotropic angle on skin friction of stress for
Newtonian fluid ($N = 0$, $f = 0$) and micropolar fluid ($N = 1$, $f = 2$)
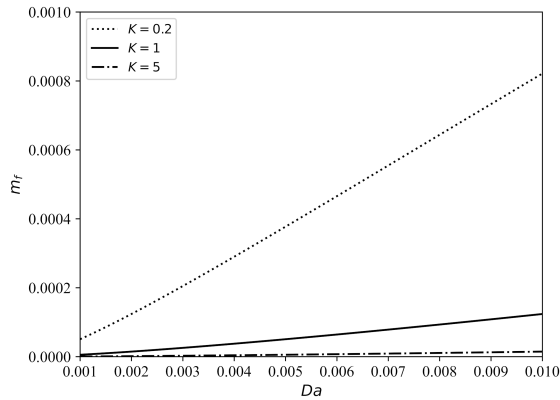on upper plate when $K = 0.25$, $\Gamma_1 = \Gamma_2 = \lambda_1 = \lambda_2 = 10$

Fig. 18. Impact of permeability ratio on skin friction of couple stress
on upper plate when $\psi = 0, N = 1, f = 2, \Gamma_1 = \Gamma_2 = \lambda_1 = \lambda_2 = 10$
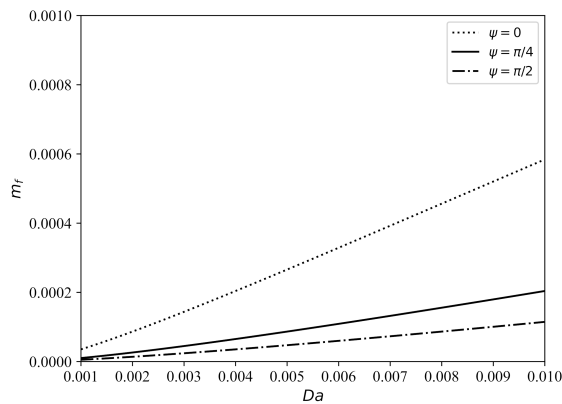

Fig. 19. Impact of anisotropic angle on skin friction of couple stress
on upper plate when $K = 0.25, N = 1, f = 2, \Gamma_1 = \Gamma_2 = \lambda_1 = \lambda_2 = 10$

4.1. Limiting cases

When $\Gamma_1, \Gamma_2 \to \infty$ and $\lambda_1, \lambda_2 \to \infty$, then it is a case of no-slip and no-spin slip, and when $N = 0$, then the micropolar fluid reduces to a classical Newtonian fluid. Then, velocity vector Eq. (24) reduces into

$$u = c_1 e^{-\eta y} + c_2 e^{\eta y} - \frac{Q}{\alpha^2}, \quad \text{where } \eta = \sqrt{\alpha^2}. \tag{29}$$

For this case, the effect of permeability ratio and anisotropic angle on fluid velocity are presented in Figs. 20 and 21. We found that our limiting case of Newtonian fluid agrees well with the result of Degan et al. [6] and Karmakar and Raja Shekhar's work [7].
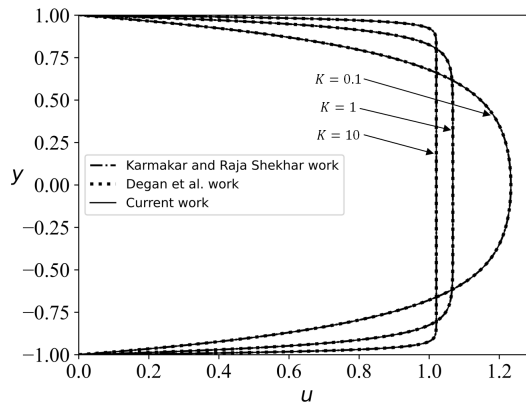
Fig. 20. Permeability ratio's influence on velocity when
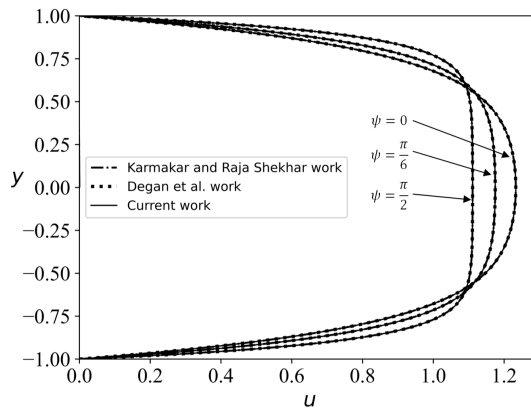$Da = 0.004, N = 0, \psi = 0$

Fig. 21. Anisotropic angle's influence on velocity when
$Da = 0.01, N = 0, K = 0.25$

If $Da \to \infty, \Gamma_1, \Gamma_2 \to \infty$, and $\lambda_1, \lambda_2 \to \infty$ then, the current problem will represent the plane-Poiseuille flow of micropolar fluid with the no-slip boundary condition. And Eq. (19) and (21) become

$$\frac{\partial^2 u_\infty}{\partial y^2} + l\frac{\partial v}{\partial y} - Q = 0, \tag{30}$$

$$\frac{\partial^2 v_\infty}{\partial y^2} - f\frac{\partial u_\infty}{\partial y} - 2f v_\infty = 0, \tag{31}$$

with the no-slip boundary conditions are

$$u_\infty = 0, \ v_\infty = 0, \quad \text{at} \ y = -1, \tag{32}$$

$$\text{and} \quad u_\infty = 0, \ v_\infty = 0, \quad \text{at} \ y = 1. \tag{33}$$

Solution of the above equations using the boundary conditions Eq. (32) and Eq. (33) are

$$u_\infty = c_1 e^{-\zeta y} + c_2 e^{\zeta y} + c_3 y + c_4 + \frac{Q y^2 f}{\zeta^2}, \tag{34}$$

$$v_\infty = \frac{\zeta}{l}(c_1 e^{-\zeta y} - c_2 e^{\zeta y}) - c_3 - \frac{Q y f}{\zeta^2}, \tag{35}$$

where

$$c_1 = -\frac{Q f l e^\zeta}{\zeta_1},$$

$$c_2 = -\frac{Q f l e^\zeta}{\zeta_1},$$

$$c_3 = 0,$$

$$c_4 = -\frac{Q f \left[(\zeta - l)e^{2\zeta} - (\zeta + l)\right]}{\zeta_1}.$$

where $\zeta = \sqrt{(2 - l) f}$, $\zeta_1 = \zeta^3 \left(e^{2\zeta} - 1\right)$.

When we put $l = 0$ in Eq. (30), then it represents the velocity profile of plane-Poiseuille flow of Newtonian fluid. Using Eq. (26), we find the value of Q for this case and that is $Q \simeq -3$. Then, the expression of velocity profile is

$$u_\infty = \frac{3}{2}(1 - y^2), \tag{36}$$

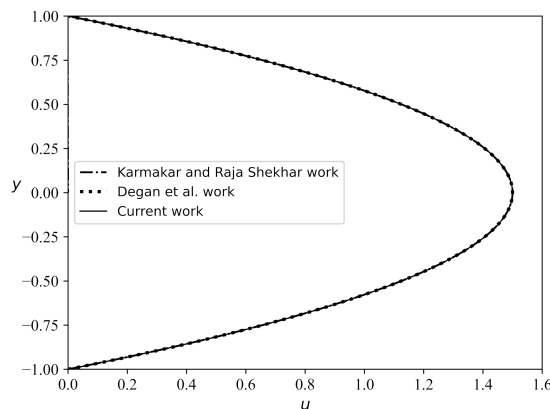Fig. 22 shows that the present work is consistent with Degan et al. [6] and Karmakar's [7] works.

Fig. 22. Velocity profile for $\mathrm{Da} \to \infty, \Gamma_1, \Gamma_2 \to \infty, \lambda_1, \lambda_2 \to \infty, N = 0$

5. Conclusions

The flow of micropolar fluid through an anisotropic porous medium between two impermeable plates and at both plates slip boundary conditions are considered for both velocity and microrotation. The impact of anisotropic permeability, micropolar parameter, slip, and spin parameters on velocity and microrotation are presented through the graphs. The main findings are listed below:

- The velocity and microrotation profiles decrease as the permeability ratio and orientation angle increase.
- The velocity slip parameters impact the velocity vector near the plates only, and the spin slip shows minor enhancement on the velocity vector but substantially impacts the microrotation vector.
- Velocity and microrotation profile increase as Darcy's number increases.
- The increasing micropolarity parameter causes a decrease in velocity and microrotation profiles.
- Skin friction increases as permeability along the flow direction increases with a decrease in the permeability ratio and the anisotropic angle.
- If we consider constant volume flow throughout any porous channel, then anisotropic nature of porous medium provide greater insight about flow than an isotropic porous medium. The pressure gradient required for flow is lowered due to the presence of slip.
- The possible applications of the present problem are in the field of the extraction of oil, blood flow through porous layer arteries, fluid flow through porous rocks, tree trunks, manmade porous lattice, etc.
- This anisotropic structure with slip condition at walls can be used to study the magnetic effect on immiscible fluid, which is widely used in porous layered arteries, in the extraction of crude oil, in the purification process, and in other engineering process.

Acknowledgements

References

[1] D.A. Nield and A. Bejan. *Convection in Porous Media*. Springer, 2017. doi: 10.1007/978-3-319-49562-0.

[2] S.I. Abdelsalam, W. Abbas, A.M. Megahed, and A.A.M. Said. A comparative study on the rheological properties of upper convected Maxwell fluid along a permeable stretched sheet. *Heliyon*, 9(12):e22740, 2023. doi: 10.1016/j.heliyon.2023.e22740.

[3] S.I. Abdelsalam and A.Z. Zaher. Biomimetic amelioration of zirconium nanoparticles on a rigid substrate over viscous slime—a physiological approach. *Applied Mathematics and Mechanics*, 44(9):1563–1576, 2023. doi: 10.1007/s10483-023-3030-7.

[4] M.M. Bhatti, K. Vafai, and S.I. Abdelsalam. The role of nanofluids in renewable energy engineering. *Nanomaterials*, 13(19):2671, 2023. doi: 10.3390/nano13192671.

[5] P.A. Tyvand and L. Storesletten. Onset of convection in an anisotropic porous medium with oblique principal axes. *Journal of Fluid Mechanics*, 226:371–382, 1991. doi: 10.1017/S0022112091002422.

[6] G. Degan, S. Zohoun, and P. Vasseur. Forced convection in horizontal porous channels with hydrodynamic anisotropy. *International Journal of Heat and Mass Transfer*, 45(15):3181–3188, 2002. doi: 10.1016/S0017-9310(02)00032-7.

[7] T. Karmakar and G.P. Raja Sekhar. Effect of anisotropic permeability on fluid flow through composite porous channel. *Journal of Engineering Mathematics*, 100(1):33–51, 2016. doi: 10.1007/s10665-015-9831-9.

[8] C. Israel-Cookey, O.A. Davies, and A.P. Ngeri. Magnetohydrodynamic forced convection and heat transfer of a Casson fluid flow in an anisotropic porous channel with isoflux boundaries. *World Journal of Advanced Research and Reviews*, 18(03):1332–1347, 2023. doi: 10.30574/w-jarr.2023.18.3.1214.

[9] A.C. Eringen. Theory of micropolar fluids. *Journal of Mathematics and Mechanics*, 16(1):1–18, 1966.

[10] T. Ariman, M.A. Turk, and N.D. Sylvester. Applications of microcontinuum fluid mechanics. *International Journal of Engineering Science*, 12(4):273–293, 1974. doi: 10.1016/0020-7225(74)90059-7.

[11] G. Łukaszewicz. *Micropolar Fluids: Theory and applications*. Springer Science & Business Media, 2012. doi: 10.1007/978-1-4612-0641-5.

[12] T. Ariman and A.S. Cakmak. Some basic viscous flows in micropolar fluids. *Rheologica Acta*, 7(3):236–242, 1968. doi: 10.1007/BF01985784.

[13] S. Nadeem, M. Hussain, and M. Naz. Mhd stagnation flow of a micropolar fluid through a porous medium. *Meccanica*, 45:869–880, 2010. doi: 10.1007/s11012-010-9297-9.

[14] S.K. Pandey and M.K. Chaube. Peristaltic flow of a micropolar fluid through a porous medium in the presence of an external magnetic field. *Communications in Nonlinear Science and Numerical Simulation*, 16(9):3591–3601, 2011. doi: 10.1016/j.cnsns.2011.01.003.

[15] K.P. Madasu and T. Bucha. MHD on a cylinder implanted in a porous media of micropolar fluid. *Journal of Theoretical and Applied Mechanics, Sofia*, 50(4):307–320, 2020. doi: 10.7546/JTAM.50.20.04.01.

[16] Ali J Chamkha. Non-Darcy hydromagnetic free convection from a cone and a wedge in porous media. *International Communications in Heat and Mass Transfer*, 23(6):875–887, 1996. doi: 10.1016/0735-1933(96)00070-X.

[17] A.J. Chamkha. Non-Darcy fully developed mixed convection in a porous medium channel with heat generation/absorption and hydromagnetic effects. *Numerical Heat Transfer, Part A: Applications*, 32(6):653–675, 1997. doi: 10.1080/10407789708913911.

[18] A.J. Chamkha. Hydromagnetic two-phase flow in a channel. *International Journal of Engineering Science*, 33(3):437–446, 1995. doi: 10.1016/0020-7225(93)E0006-Q.

[19] A.J. Chamkha. Unsteady laminar hydromagnetic fluid–particle flow and heat transfer in channels and circular pipes. *International Journal of Heat and Fluid Flow*, 21(6):740–746, 2000. doi: 10.1016/S0142-727X(00)00031-X.

[20] A.J. Chamkha, T. Groşan, and I. Pop. Fully developed free convection of a micropolar fluid in a vertical channel. *International Communications in Heat and Mass Transfer*, 29(8):1119–1127, 2002. doi: 10.1016/S0735-1933(02)00440-2.

[21] A.J. Chamkha. On laminar hydromagnetic mixed convection flow in a vertical channel with symmetric and asymmetric wall heating conditions. *International Journal of Heat and Mass Transfer*, 45(12):2509–2525, 2002. doi: 10.1016/S0017-9310(01)00342-8.

[22] A.J. Chamkha. Flow of two-immiscible fluids in porous and nonporous channels. *Journal of Fluids Engineering*, 122(1):117–124, 2000. doi: 10.1115/1.483233.

[23] J.C. Umavathi, A.J. Chamkha, A. Mateen, and A. Al-Mudhaf. Unsteady two-fluid flow and heat transfer in a horizontal channel. *Heat and Mass Transfer*, 42(2):81–90, 2005. doi: 10.1007/s00231-004-0565-x.

[24] J.P. Kumar, J.C. Umavathi, A.J. Chamkha, and I. Pop. Fully-developed free-convective flow of micropolar and viscous fluids in a vertical channel. *Applied Mathematical Modelling*, 34(5):1175–1186, 2010. doi: 10.1016/j.apm.2009.08.007.

[25] M. Keimanesh, M.M. Rashidi, A.J. Chamkha, and R. Jafari. Study of a third grade non-Newtonian fluid flow between two parallel plates using the multi-step differential transform method. *Computers & Mathematics with Applications*, 62(8):2871–2891, 2011. doi: 10.1016/j.camwa.2011.07.054.

[26] M. Kocić, Ž Stamenković, J. Petrović, and J. Bogdanović-Jovanović. MHD micropolar fluid flow in porous media. *Advances in Mechanical Engineering*, 15(6):1–18, 2023. doi: 10.1177/16878132231178436.

[27] S.E. Ahmed and A.M. Rashad. Natural convection of micropolar nanofluids in a rectangular enclosure saturated with anisotropic porous media. *Journal of Porous Media*, 19(8):737–750, 2016. doi: 10.1615/JPorMedia.v19.i8.60.

[28] C.L.M.H. Navier. Memoirs de l'Academie. *Royale des Sciences de l'Institut de France*, 1:414–416, 1823.

[29] P.A. Thompson and S.M. Troian. A general boundary condition for liquid flow at solid surfaces. *Nature*, 389(6649):360–362, 1997. doi: 10.1038/38686.

[30] C. Neto, D.R. Evans, E. Bonaccurso, H.J. Butt, and V.S.J. Craig. Boundary slip in Newtonian liquids: a review of experimental studies. *Reports on Progress in Physics*, 68(12):2859, 2005. doi: 10.1088/0034-4885/68/12/R05.

[31] S.G. Hatzikiriakos. Wall slip of molten polymers. *Progress in Polymer Science*, 37(4):624–643, 2012. doi: 10.1016/j.progpolymsci.2011.09.004.

[32] H.A. Stone, A.D. Stroock, and A. Ajdari. Engineering flows in small devices: microfluidics toward a lab-on-a-chip. *Annual Review of Fluid Mechanics*, 36:381–411, 2004. doi: 10.1146/annurev.fluid.36.050802.122124.

[33] K. Ramesh. Influence of heat transfer on Poiseuille flow of MHD Jeffrey fluid through porous medium with slip boundary conditions. *AIP Conference Proceedings*, 1860(1):020044, 2017. doi: 10.1063/1.4990343.

[34] J. Chen, S.M. Han, and W.R. Hwang. Effective Navier-slip in non-Newtonian fluid flows over corrugated surfaces. *Physics of Fluids*, 32(11):113103, 2020. doi: 10.1063/5.0027079.

[35] S.A. Slayi and E.A. Ashmawy. State space solution to the unsteady slip flow of a micropolar fluid between parallel plates. *International Journal of Scientific and Innovative Mathematical Research*, 2(10):827–836, 2014.

[36] K.P. Madasu and P. Sarkar. Couple stress fluid past a sphere embedded in a porous medium. *Archive of Mechanical Engineering*, 69(1):5–19, 2022. doi: 10.24425/ame.2021.139314.

[37] T. Bucha and K.P. Madasu. Slow flow past a weakly permeable spheroidal particle in a hypothetical cell. *Archive of Mechanical Engineering*, 68(2):119–146, 2021. doi: 10.24425/ame.2021.137044.

[38] J. Lu, H.K. Jang, S.B. Lee, and W.R. Hwang. Characterization on the anisotropic slip for flows over unidirectional fibrous porous media for advanced composites manufacturing. *Composites Part A: Applied Science and Manufacturing*, 100:9–19, 2017. doi: 10.1016/j.compositesa.2017.04.021.

[39] T. Karmakar. Physics of unsteady Couette flow in an anisotropic porous medium. *Journal of Engineering Mathematics*, 130(1):8, 2021. doi: 10.1007/s10665-021-10165-9.

[40] H.H. Sherief, M.S. Faltas, and S. El-Sapa. Pipe flow of magneto-micropolar fluids with slip. *Canadian Journal of Physics*, 95(10):885–893, 2017. doi: 10.1139/cjp-2016-0508.

[41] H.N.G. Wadley, N.A. Fleck, and A.G. Evans. Fabrication and structural performance of periodic cellular metal sandwich structures. *Composites Science and Technology*, 63(16):2331–2343, 2003. doi: 10.1016/S0266-3538(03)00266-5.

[42] V.S. Deshpande, N.A. Fleck, and M.F. Ashby. Effective properties of the octet-truss lattice material. *Journal of the Mechanics and Physics of Solids*, 49(8):1747–1769, 2001. doi: 10.1016/S0022-5096(01)00010-2.

[43] D.T. Queheillalt and H.N.G. Wadley. Cellular metal lattices with hollow trusses. *Acta Materialia*, 53(2):303–313, 2005. doi: 10.1016/j.actamat.2004.09.024.

[44] L.-P. Lefebvre, J. Banhart, and D.C. Dunand. Porous metals and metallic foams: current status and recent developments. *Advanced Engineering Materials*, 10(9):775–787, 2008. doi: 10.1002/adem.200800241.

[45] B.C. Tappan, S.A. Steiner III, and E.P. Luther. Nanoporous metal foams. *Angewandte Chemie International Edition*, 49(27):4544–4565, 2010. doi: 10.1002/anie.200902994.